Dear author,

Please note that changes made in the online proofing system will be added to the article before publication but are not reflected in this PDF.

We also ask that this file not be used for submitting corrections.

A fast and general method to empirically estimate the complexity of brain responses to transcranial and intracranial stimulations

Renzo Comolatti [a], Andrea Pigorini [b], Silvia Casarotto [b], Matteo Fecchio [b], Guilherme Faria [a], Simone Sarasso [b], Mario Rosanova [b], Olivia Gosseries [c, d], Mélanie Boly [e], Olivier Bodart [c, d], Didier Ledoux [c], Jean-François Brichant [f], Lino Nobili [g, h], Steven Laureys [c, d], Giulio Tononi [e], Marcello Massimini [b, i, 1], Adenauer G. Casali [a, *, 1]

[a] Institute of Science and Technology, Federal University of São Paulo, São José dos Campos, 12231-280, Brazil
[b] Department of Biomedical and Clinical Sciences "Luigi Sacco", University of Milan, Milan, 20157, Italy
[c] GIGA-Consciousness, GIGA Research, University of Liège, Liège, 4000, Belgium
[d] Coma Science Group, University Hospital of Liège, Liège, 4000, Belgium
[e] Department of Psychiatry, University of Wisconsin, Madison, 53719, USA
[f] Department of Anesthesia and Intensive Care Medicine, University Hospital of Liège, Liège, 4000, Belgium
[g] Center of Epilepsy Surgery "C. Munari", Department of Neuroscience, Niguarda Hospital, Milan, 20162, Italy
[h] Child Neuropsychiatry, IRCCS G. Gaslini, DINOGMI, University of Genoa, Genova, 16147, Italy
[i] Istituto Di Ricovero e Cura a Carattere Scientifico, Fondazione Don Carlo Gnocchi, Milan, 20148, Italy

ARTICLE INFO

ABSTRACT

Background: The Perturbational Complexity Index (PCI) was recently introduced to assess the capacity of thalamocortical circuits to engage in complex patterns of causal interactions. While showing high accuracy in detecting consciousness in brain-injured patients, PCI depends on elaborate experimental setups and offline processing, and has restricted applicability to other types of brain signals beyond transcranial magnetic stimulation and high-density EEG (TMS/hd-EEG) recordings.
Objective: We aim to address these limitations by introducing PCIST, a fast method for estimating perturbational complexity of any given brain response signal.
Methods: PCIST is based on dimensionality reduction and state transitions (ST) quantification of evoked potentials. The index was validated on a large dataset of TMS/hd-EEG recordings obtained from 108 healthy subjects and 108 brain-injured patients, and tested on sparse intracranial recordings (SEEG) of 9 patients undergoing intracranial single-pulse electrical stimulation (SPES) during wakefulness and sleep.
Results: When calculated on TMS/hd-EEG potentials, PCIST performed with the same accuracy as the original PCI, while improving on the previous method by being computed in less than a second and requiring a simpler set-up. In SPES/SEEG signals, the index was able to quantify a systematic reduction of intracranial complexity during sleep, confirming the occurrence of state-dependent changes in the effective connectivity of thalamocortical circuits, as originally assessed through TMS/hd-EEG.
Conclusions: PCIST represents a fundamental advancement towards the implementation of a reliable and fast clinical tool for the bedside assessment of consciousness as well as a general measure to explore the neuronal mechanisms of loss/recovery of brain complexity across scales and models.

© 2019 Elsevier Inc. All rights reserved.

Introduction

Measures of brain complexity have recently begun to move from the realm of theoretical neuroscience [1–6] into the field of experimental neurophysiology to study differences between global brain states, from wakefulness to sleep and anesthesia [7–10]. Further, measures of brain complexity have been considered as

useful paraclinical indices to assess consciousness at the bedside of brain-injured patients [11–15]. In this spirit, a novel strategy based on quantifying the global effects of direct cortical perturbations was recently introduced [16]. This approach is motivated by the general theoretical principle that a brain's capacity for consciousness relies on its ability to integrate information [5]. In this perspective, a critical mechanism supporting the emergence of conscious experience is the ability of different neural elements to engage in complex patterns of causal interactions such that the whole system generates information over and above its parts.

Practically, in order to estimate the amount of causal, irreducible information that a system can generate, a general procedure was implemented based on two steps: (i) locally perturbing the system in a controlled and reproducible way to trigger a cause-effect chain and (ii) quantifying the spatiotemporal complexity of the ensuing deterministic response to estimate information. The original implementation of this perturb-and-measure approach [16] involved (i) stimulating the brain with transcranial magnetic stimulation (TMS) and (ii) computing the algorithmic (Lempel-Ziv) complexity of the resulting patterns of activations at the level of cortical sources derived from the inverse solution of high-density electroencephalographic (hd-EEG) responses; this metric will be henceforth referred to as Lempel-Ziv Perturbational Complexity Index (PCI^{LZ}).

Albeit macroscopic and coarse, PCI^{LZ} provided maximum (100%) accuracy in detecting consciousness in a large (n = 150) benchmark population of subjects who could confirm the presence or absence of conscious experience through immediate or delayed reports [17]. PCI^{LZ} was lower in all unresponsive subjects who did not report any conscious experience upon awakening from NREM sleep or midazolam, xenon, and propofol anesthesia, and was invariably higher for subjects in which consciousness was present, including awake controls, conscious brain-injured patients and subjects who were disconnected and unresponsive during dreaming and ketamine anesthesia but retrospectively reported having had vivid conscious experiences upon awakening [17,18]. Once calibrated on the gold-standard of subjective reports, PCI^{LZ} measurements performed at the bedside of non-communicating subjects with brain injuries offered high sensitivity (94%) in detecting minimally conscious patients and allowed identifying a significant percentage (about 20%) of vegetative state/unresponsive wakefulness syndrome (VS/UWS) cases with high brain complexity, who had a higher chance of eventually recovering consciousness [17].

While PCI^{LZ} performs with unprecedented accuracy, it also has practical drawbacks and limitations. First, PCI^{LZ} can only be computed on spatiotemporal matrices of cortical activations that are obtained after an intensive processing of TMS/hd-EEG data, including forward modeling [19], source estimation [20] and permutation-based statistics at the single-trial level. All these steps imply a complicated and lengthy off-line analysis pipeline that hinders the dissemination of the method and its application as a routine clinical bedside tool. Clearly, the possibility of estimating perturbational complexity directly at the level of EEG sensors may have critical advantages: not only it would render the analysis process faster (ideally, on-line), easier to standardize and immune to the technical caveats of source modeling, but it would also allow the use of simplified and cheaper set-ups (i.e. not requiring hd-EEG and subject-specific MRI scans).

A second important drawback of PCI^{LZ} is its limited application to signals other than TMS/hd-EEG evoked potentials. Intracranial single-pulse electrical stimulation (SPES) combined with local field potential (LFP) recordings in human [21,22] and animal models [23–26], as well as intra and extracellular responses recorded from cortical slices [27,28], offer an unprecedented range of opportunities to validate and interpret TMS-EEG results and to elucidate the

relationships between neuronal dynamics, network complexity and consciousness [29]. However, because PCI^{LZ} relies on EEG source estimation, its extension to other types of recordings, such as sparse matrices of intracranial stereo EEG (SEEG) recordings and in vivo/in vitro LFP, is not straightforward.

Here we address these limitations and propose a novel measure of perturbational complexity that bears conceptual similarities with PCI^{LZ} but is much faster to compute and in principle generalizable to any type of evoked brain signal. Conceptually, we started from the notion that the binary sequences of activation and deactivations which are compressed by PCI^{LZ} can be considered as sequences of transitions between different states: a "response state" and a "non-response" or "baseline state" [30]. Thus, one should expect to find high values of perturbational complexity in systems that react to the initial perturbation by exhibiting multiple and irreducible patterns of transitions between response and non-response states.

Following this intuition, we developed PCI^{ST}, an index that combines dimensionality reduction and a novel metric of recurrence quantification analysis (RQA) to empirically quantify perturbational complexity as the overall number of non-redundant state transitions (ST) caused by the perturbation. In this paper, we specifically aimed at (i) validating PCI^{ST} as a practical tool for detecting consciousness at the bedside, and (ii) demonstrating its generalizability from transcranial (TMS/EEG) to intracranial (SPES/SEEG) stimulation and recordings. Hence, we first tested PCI^{ST} on a large dataset encompassing 719 TMS/hd-EEG sessions recorded from healthy subjects during wakefulness, non-rapid eye movement (NREM) sleep and anesthesia as well as brain-injured patients with disorders of consciousness (DOC). To the second aim, we tested PCI^{ST} ability to capture state-dependent changes in brain complexity on 84 SEEG recordings obtained in epileptic patients undergoing intracranial single-pulse electrical stimulation (SPES) for pre-surgical evaluation during both wakefulness and sleep.

Material and methods

Participants

Healthy subjects

The benchmark dataset consisted of 382 TMS/hd-EEG sessions reported in previous works [16,17,31]. Data were recorded from 108 healthy subjects (female, n = 63; age range = 18–80 years) in two conditions (see Fig. S1, panel A for further information about the number of sessions and subjects for each protocol): (1) while they were unresponsive and did not provide any subjective report upon awakening (NREM sleep, n = 19; midazolam sedation at anesthetic concentrations, n = 6; anesthesia with xenon, n = 6; anesthesia with propofol, n = 6) and (2) while they were awake and able to provide an immediate subjective report (n = 103, including 32 subjects also recorded in the previously described unresponsive conditions). Protocols and informed consents were approved by the local ethical committees [16,17,31].

Brain-injured patients

TMS/hd-EEG data were also obtained in a population of 108 brain-injured patients (95 reported in a previous work [17]) with newly acquired data recorded following the same previously reported protocol [17], totalizing 337 TMS/hd-EEG sessions (Fig. S1, panel B). Sixteen brain-injured patients were conscious and encompassed 5 individuals affected by locked-in syndrome (LIS) and 11 individuals who emerged from minimally conscious state (EMCS) by recovering functional communication and/or functional use of objects after a previous DOC. The remaining 92 brain-injured

patients had a severe DOC and were repeatedly evaluated with the Coma Recovery Scale-Revised (CRS-R) for a period of 1 week (4 times, every other day). Patients showing only reflexive behavior across all evaluations were considered as being unresponsive (Unresponsive Wakefulness Syndrome, UWS, 43 patients), whereas patients showing signs of nonreflexive behaviors in at least one evaluation were considered as minimally conscious (Minimally Conscious State, MCS, 49 patients). Protocols and informed consents were approved by the local ethical committees [17] and written informed consent was obtained from healthy subjects, from communicative patients, and from legal surrogates of DOC patients.

Epileptic patients

Data included in the present study derived from a dataset collected during the pre-surgical evaluation of nine (eight previously reported [22]) neurosurgical patients with a history of drug-resistant, focal epilepsy. All subjects were candidates for surgical removal of the epileptic focus. During the pre-surgical evaluation all patients underwent individual investigation with SPES and simultaneous SEEG recordings for mapping eloquent areas and for precisely identifying the epileptogenic cortical network [32–35]. The investigated hemisphere, the duration of implantation and the location and number of stimulation sites were determined based on the non-invasive clinical assessment. The stimulation, recording and data treatment procedures were approved by the local ethical committee [22]. All patients provided written informed consent.

TMS/hd-EEG measurements and data analysis

Specific protocols for acquiring and analyzing TMS/hd-EEG potentials were described in Refs. [16,17]. In brief, data were recorded with a 60-channel TMS-compatible EEG amplifier and MRI-guided TMS pulses were delivered with a focal biphasic stimulator. A noise masking sound tailored to the specific coil was played through inserted earphones and titrated by subjects within safety limits (<85 dB). In each subject, multiple sessions of ~200 stimuli were collected with TMS targeted to different areas at different intensities accordingly to the specific protocol. EEG responses to TMS were visually inspected to reject single trials and channels with bad signal quality. Independent component analysis was applied to remove residual artifactual components resulting from eye movements and muscle activations. Bad channels were then interpolated using spherical interpolation and data were bandpass filtered (0.1–45 Hz), downsampled to 725 Hz, segmented between −400 and 400 ms, re-referenced to the average, baseline corrected (−400 to −5 ms) and averaged across trials.

Intracranial measurements and data analysis

The procedures for SEEG data acquisition and analysis are described in Ref. [22]. Briefly, intracranial activity was recorded at 1000 Hz using a 192-channel recording system (Nihon-Kohden Neurofax-110) during electrical stimulation applied through one pair of adjacent contacts at different locations. SPES/SEEG sessions were obtained from all nine patients both during wakefulness and NREM sleep, resulting in a total of 84 sessions (see Table S1 and Fig. S2 for contact locations). The location of the bipolar contacts was assessed by post-implantation tomographic imaging (CT) scans and Freesurfer reconstruction [36] of the individual brains confirmed using the Destrieux ATLAS [37]. The analysis was performed only in those recordings in which the stimulating bipolar contacts (i) pertained to the same cortical anatomical structure, (ii) were far from the epileptogenic zone and/or cortical lesions, (iii) did not evoke epileptic responses either in wakefulness or NREM, and without alterations of the cortical tissue [38], (iv) did

not elicit muscle twitches, sensations or evident motor/cognitive effects, (v) occurred during a period of wakefulness or N3 sleep (without disrupting sleep depth). We further excluded from analysis contacts located in the epileptogenic zone and/or in cortical lesions, as well as those showing epileptiform activity as assessed by visual inspection (remaining contacts averaged 69.31 ± 15.31). Trials showing pathological activity [38] were detected by visual inspection and excluded from the analysis and SPES-evoked responses were computed by averaging the remaining trials. Data were referenced to a contact located entirely in the white matter, subjected to linear detrend and bandpass filtering (0.5–300 Hz) and bipolar montages were calculated by subtracting the signals from adjacent contacts of the same depth-electrode [39,40]. Stimulation artifact was reduced by applying a Tukey-windowed median filtering [41] between −5 and 5 ms. Data were segmented between −300 and 600 ms and the SEEG magnitude at each electrode was computed as a z-score relative to its baseline.
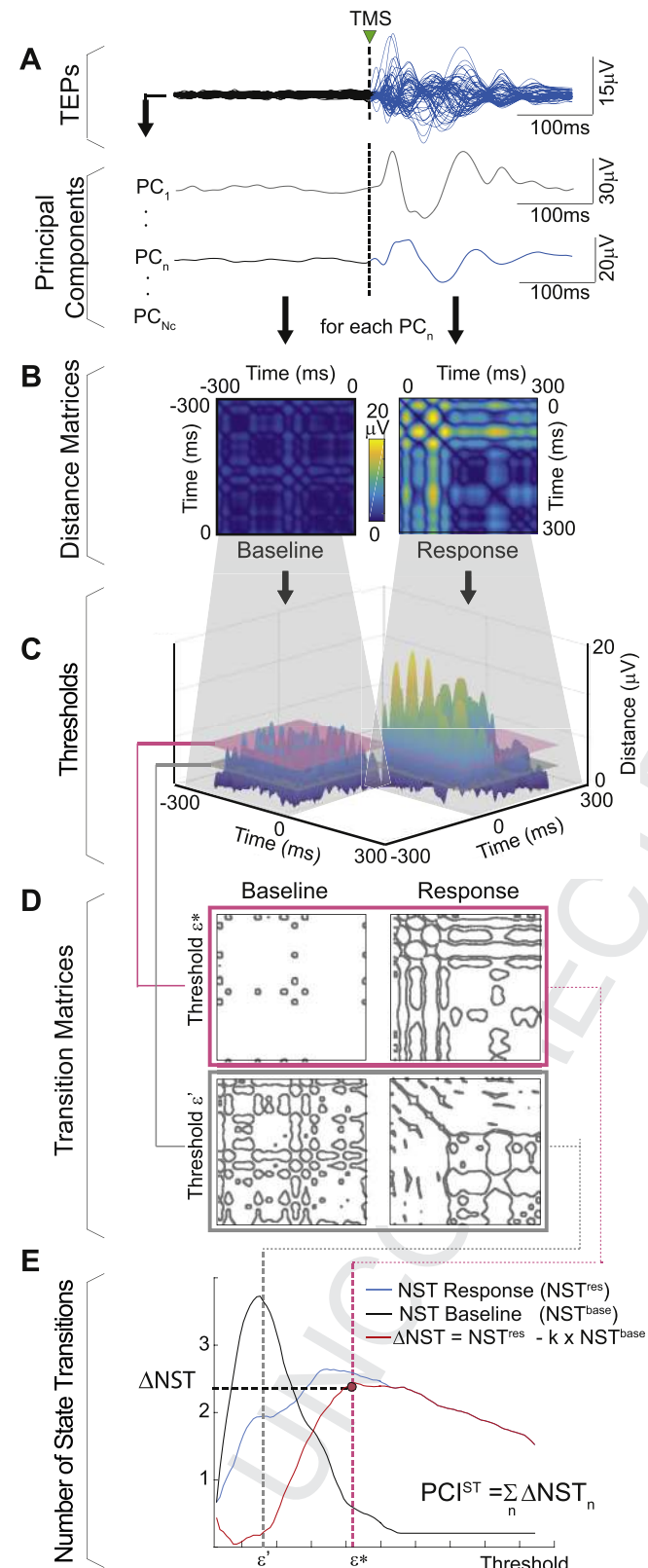
Perturbational complexity index based on state transitions (PCI^{ST})

In its original formulation [16], perturbational complexity was calculated by binarizing TMS-evoked potentials (TEPs) at the estimated cortical source level using a fixed threshold derived from non-parametric statistics with respect to the baseline (pre-stimulus) and subsequently compressing the binary spatiotemporal patterns with the Lempel-Ziv algorithm. An underlying assumption of this strategy is that complex activations engaged by the perturbation appear on the evoked signals as patterns of oscillations around a fixed amplitude scale. Although proven successful when applied at the source level, this approach was less sensitive in detecting complexity when calculated directly at the EEG-scalp level, where fast oscillations are more likely to appear on top of larger and slower envelopes as result of increased volume conduction and signal mixing (Fig. S3). Furthermore, complex neuronal oscillations occurring in amplitude scales that are not determined by a fixed threshold can also be observed in microscopic and mesoscopic recordings due to cross-frequency couplings [42–46], and a binarized measure applied to such scales would have limited applicability to detect complex physiological activations.

Aiming at a general index of perturbational complexity that can be fast and efficiently calculated directly at the EEG-sensors level, we here took a non-binary approach and quantified the spatio-temporal complexity of evoked potentials by exploring multiple amplitude fluctuations present in principal components of the response. Starting from trial-averaged signals recorded in response to a perturbation, singular value decomposition was performed in order to effectively reduce the dimension of the data (Fig. 1A). The principal components were selected so as to account for at least 99% of the response strength measured in terms of the square mean field power and components with low signal-to-noise ratio were further removed.

The complexity of each resulting principal component was then evaluated using a method derived from RQA [30,47,48] by quantifying what we call *state transitions*. More specifically, distance matrices, defined by the voltage-amplitude distances between all time-points of the signal, were calculated separately for pre-stimulus and post-stimulus samples (Fig. 1B). Next, these distance matrices were thresholded at a given scale ε (Fig. 1C), yielding corresponding transition matrices (Fig. 1D), i.e. contour plots that depicts the temporal transitions between states − roughly, the ups and downs in the signal −, for both the baseline and the response. By varying the threshold ε and comparing the average number of state transitions (NST) in the matrices of the response with that of the baseline, we looked for the scales at which the state transitions

Fig. 1. Calculating the Perturbational complexity index based on state transitions (PCI^ST) from TMS/hd-EEG evoked potentials (TEP). PCIST is calculated by performing five steps: A) TEPs (butterfly plot, top) are decomposed in N_c principal components (PC) based on the singular value decomposition of the response to the perturbation. B) For each single component (PC$_n$, highlighted) amplitude distances are calculated between every baseline samples (black trace in A) and between every response sample (blue trace in A), resulting in a baseline and a response distance matrix, respectively. C)

in the signal's response were over and above the transitions present in the baseline activity. In this way, the complexity of the nth component (ΔNST_n) was defined as the maximized weighted difference of NST between response (NST$_n^{res}$) and baseline (NST$_n^{base}$) signals:

$$\Delta NST_n = T_R \left[NST_n^{res}(\varepsilon_n^*) - k \times NST_n^{base}(\varepsilon_n^*) \right] \quad (1)$$

Where ε_n^* is the threshold value which maximizes the weighted difference of NST (red dot in Fig. 1E) and T_R is the number of samples in the response, a normalizing factor that yields a quantity that is extensive with the length of the signal's response and largely independent of the sampling rate (Fig. S4). The parameter k was introduced to control the relative weight between pre and post-stimulus state transitions.

Finally, PCIST was defined as the sum of these maximized significant state transitions (ΔNST_n) across all selected principal components ($n = 1 \dots N_C$) of the evoked signal:

$$PCI^{ST} = \sum_{n=1}^{N_C} \Delta NST_n \quad (2)$$

An intuitive way to look at the metric is as the product between the number of principal components surviving dimensionality reduction (N_C) and the average number of state transitions across components ($\overline{\Delta NST}$), i.e. $PCI^{ST} = N_C \times \overline{\Delta NST}$. The former quantity can be regarded as a measure of the *spatial differentiation* of the brain's response to the perturbation, while the latter corresponds to the average *temporal complexity* present in the individual principal components as measured by the quantification of state transitions. As such, PCIST captures the spatiotemporal complexity of a brain response as the joint presence of spatial differentiation (N_C) and temporal complexity ($\overline{\Delta NST}$) (Fig. S5).

By its definition, PCIST is high when there are multiple linearly independent components in a spatially distributed response (spatial differentiation), each one of them contributing with significant amounts of state transitions (temporal complexity). Conversely, PCIST is expected to be low either if the perturbation evokes a strongly correlated response across different spatial recordings or if the independent components carry few temporal transitions in the response as compared to the baseline (see Supplementary Material for a detailed definition of the measure, including computational steps and parameter choice). Code for computing PCIST is available at github.com/renzocom/PCIst.

Statistical analysis

Data are presented as mean ± standard deviation (SD), and p-values less than 0.01 were considered significant. Wilcoxon-ranksum test was used for evaluating the discrimination between conscious and unconscious conditions. The classification power of discriminating different levels of consciousness was quantified by the area under the receiver operating characteristic (ROC) curve (AUC).

These matrices are then thresholded at several scales. Two scale values are depicted in the figure: a lower threshold (ε') and a higher threshold (ε^*). D) At each scale, the corresponding transition matrices are computed for both baseline and response. These matrices are used to calculate the average number of state transitions (NST) in the baseline NST^{base} and in the response NST^{res}. E) The complexity of the selected component is defined as the maximum weighted difference between the number of state transitions in the response and in the baseline (ΔNST_n). The final measure PCIST is calculated by summing the ΔNST_n values across all N_c principal components. (For interpretation of the references to colour in this figure legend, the reader is referred to the Web version of this article.)
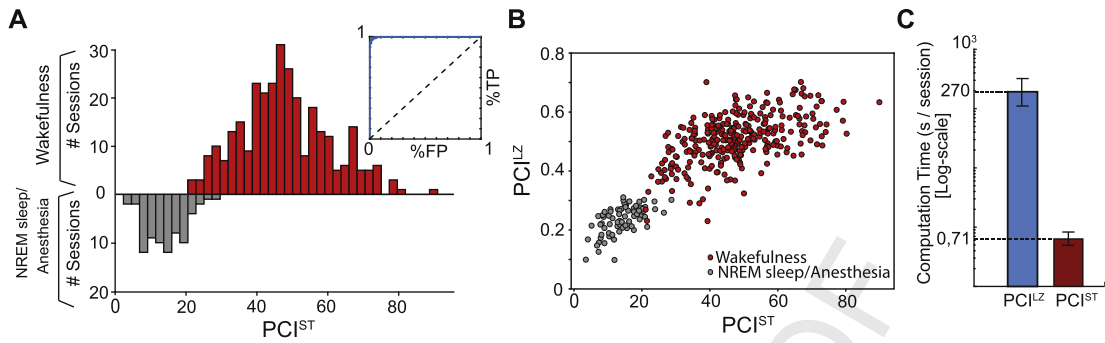
Fig. 2. PCIST discriminates between consciousness and unconsciousness in healthy individuals and is faster than PCI^{LZ}. (A) Histogram of PCIST values (left) for all 382 TMS sessions obtained from healthy individuals in the conscious (red) and unconscious (grey) conditions, with the corresponding ROC curve of the distributions (right). (B) Correlation between PCIST and PCI^{LZ} values in the benchmark dataset for conscious (red) and unconscious (grey) conditions (r = 0.82, p < 10^{-95}). (C) Mean computation time per TMS/hd-EEG session for PCIST (red) and PCI^{LZ} (blue) calculated on the benchmark dataset. (For interpretation of the references to colour in this figure legend, the reader is referred to the Web version of this article.)

Results and discussion

### PCIST is reliable and fast in benchmark conditions

PCIST was calculated on a benchmark of 382 TEPs obtained in a group of 108 healthy subjects during conscious (alert wakefulness) and unconscious (NREM sleep and anesthesia) conditions (Fig. 2A, see also Figs. S1–A for individual PCIST values). The wakefulness group presented significantly higher and more variable PCIST values (mean ± SD, 47.89 ± 12.65) than the NREM sleep/anesthesia group (14.19 ± 5.26, P = 4.7 × 10^{-40}). In terms of classification performance between conscious and unconscious conditions, PCIST showed a high classification power that was equivalent to the performance of the original version of PCI in this same dataset [17] (AUC for PCIST = 0.998, AUC for PCI^{LZ} = 0.995). Indeed, when values for each TMS/hd-EEG session were compared, we found a significant linear correlation between the metrics (r = 0.82, p < 10^{-95}, Fig. 2B). This high accuracy of PCIST in assessing consciousness was found to be stable across parameters values and robust to variations in the benchmark population (see Fig. S6). Further, in line with the general principles behind perturbational complexity, both the spatial differentiation and the temporal complexity of the TMS/EEG response were necessary to achieve this performance (Fig. S5).

Finally, because PCIST estimates perturbational complexity without employing source localization and surrogate techniques, PCIST computation was approximately 380 times faster than with PCI^{LZ}. While for a single session PCI^{LZ} took about 300 seconds to compute (270s ± 99), PCIST could be calculated in less than one second (0.71 ± 0.20, p < 10^{-127}) (Fig. 2C).

PCIST allows a simple and fast set-up at the bedside of patients

We next tested the performance of PCIST in brain-injured patients. First, an empirical threshold for discriminating consciousness from unconsciousness was extracted from all PCIST values of the benchmark population using a linear classifier [49]. This empirical cutoff was then applied to PCIST values obtained from a group of 108 brain-injured patients who had recovered from coma and evolved toward various clinical conditions. Following the previous approach [17], we classified each patient using his maximum PCIST value obtained across all recorded sessions. This approach is aimed at assessing the patient's best capacity for consciousness and parallels the diagnostic use of the best behavioral (CRS-R) score.

The sensitivity of PCIST in detecting signs of consciousness in brain-injured patients was comparable to PCI^{LZ} [17] (Fig. 3A, top): PCIST made no erroneous classifications on conscious (LIS/EMCS) patients and achieved 91.9% sensitivity among minimally conscious
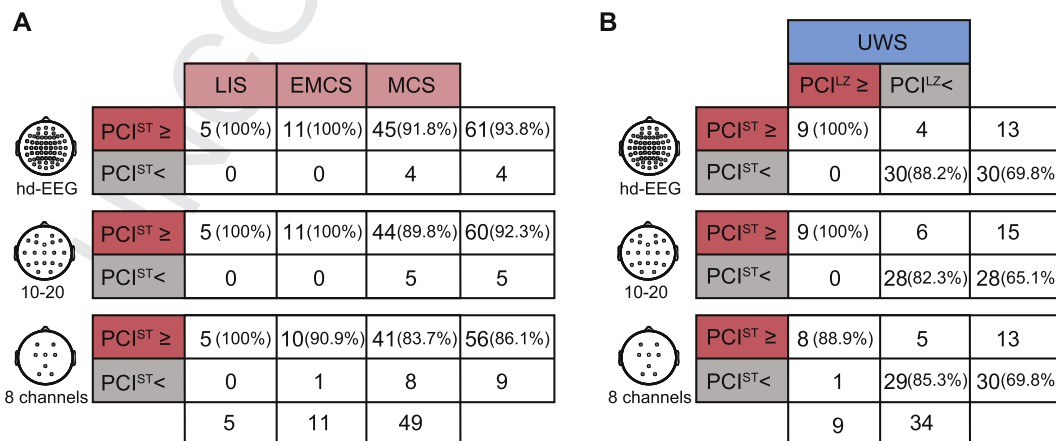

Fig. 3. PCIST's ability to detect consciousness in brain-injured patients is preserved in simpler EEG set-ups. Number and percentages of patients classified as high (PCIST≥) and low (PCIST<) complexity with respect to the corresponding classification cutoffs obtained from the benchmark dataset are shown for EEG setups of 60 (top), 19 (middle) and 8 (bottom) channels. (A) PCI$^{ST'}$ sensitivity in detecting signs of consciousness in conscious (EMCS/LIS) and minimally conscious (MCS) patients. (B) Contingency tables for the stratification of UWS patients in low complexity (PCI<) and high complexity (PCI≥) subgroups accordingly to PCI^{LZ} and PCIST.

individuals, correctly detecting signs of consciousness in 45 from 49 MCS patients (see Figs. S1–B for individual PCIST values). Cross-validation analysis confirmed the effectiveness in classifying healthy subjects and brain-injured patients with a fixed threshold extracted from the benchmark population (see Fig. S7 for computational details on the classifier used to obtain the empirical threshold and its cross-validated performance on healthy individuals and patients).

From a practical perspective, the potential of PCI to be employed as an index of consciousness in a clinical setting is significantly limited by the use of hd-EEG, which, besides entailing more expensive hardware, involves a cumbersome and lengthy preparation. While PCI^{LZ} necessarily demands hd-EEG systems so as to accurately perform source localization, PCIST can in principle be calculated on a reduced number of channels. We thus compared the performance of the index on the original hd-EEG system (60 channels) to reduced setups containing 19 and 8 electrodes (see Supplementary Material for further details). Notably the performance of the index diminished only slightly with the use of the standard 10−20 EEG system (19 channels), yielding sensitivities of 100% and 89.8% (44/49) for EMCS/LIS and MCS respectively (Fig. 3A, middle). Finally, the simpler 8-channels setup resulted in reduced sensitivity scores on both EMCS/LIS (94%) and MCS (84%) patients (Fig. 3A, bottom). An equivalent performance in discriminating
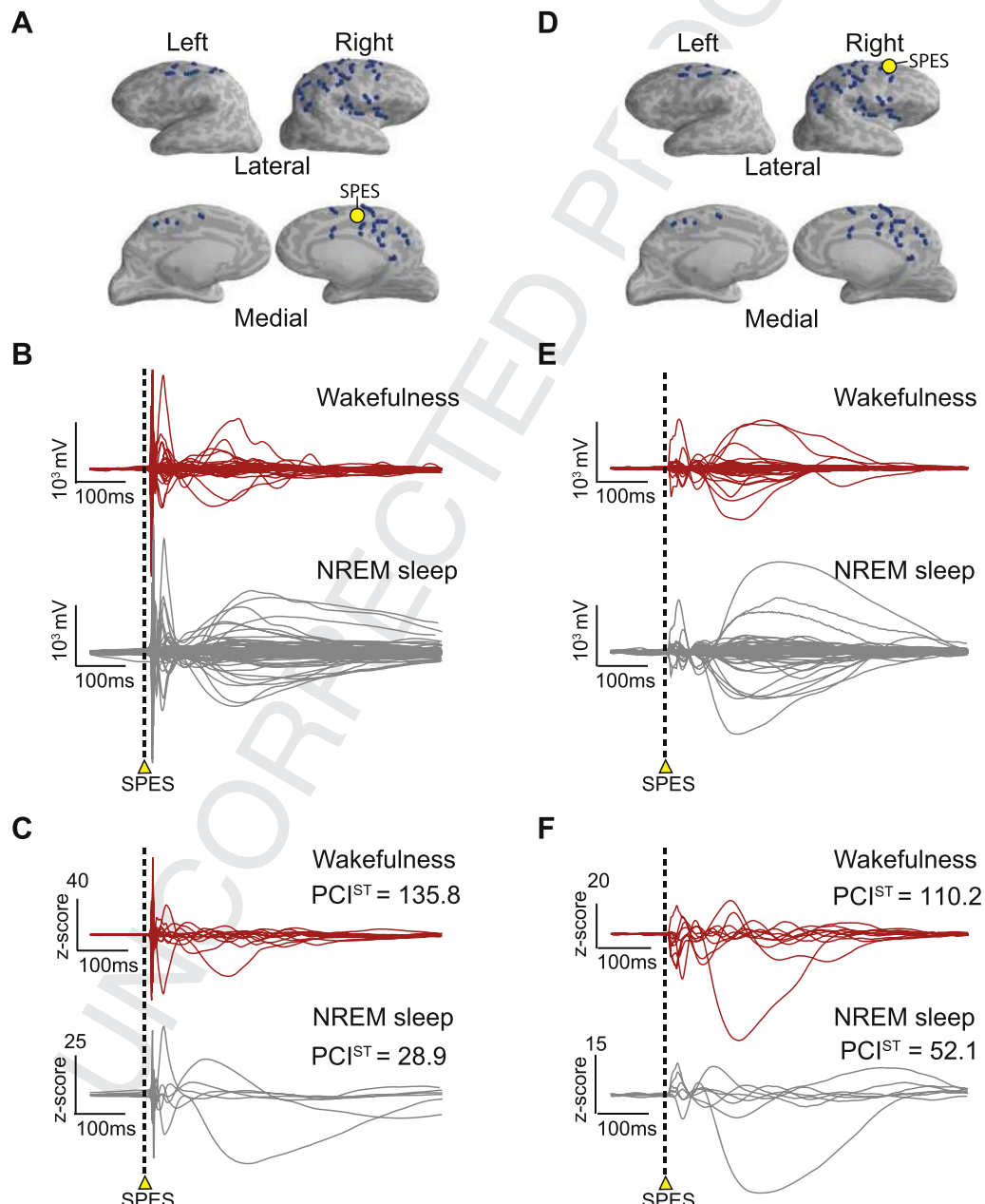

Fig. 4. **PCIST is able to quantify the spatiotemporal complexity of stereotactic EEG responses to SPES.** SPES-evoked responses in the SEEG and principal component space are shown for a representative subject during stimulation delivered on the Superior Frontal Gyrus (panels A, B, C) and on the Superior Frontal Sulcus (panels D, E, F). Panels A and D depict the positions of the stimulating contact (yellow) and remaining SEEG contacts (blue) over a brain surface reconstructed from the individual's brain. The correspondent SPES/SEEG-evoked responses are shown in the respective middle panels (B and E) as the superposition of the averaged SPES-evoked potentials recorded from all SEEG contacts during wakefulness (red traces) and NREM sleep (grey traces). Lower panels (C and F) depict the correspondent PCIST values and the normalized SPES-evoked responses decomposed in principal components after dimensionality reduction. (For interpretation of the references to colour in this figure legend, the reader is referred to the Web version of this article.)

conscious from unconscious conditions using simpler set-ups was also observed in the benchmark dataset (see Figs. S4–C and Fig. S8).

In UWS patients, brain-based measures that do not require subject's interaction with the external environment can be useful to detect a covert capacity for consciousness. In a previous study, PCI^{LZ} detected conscious-like complexity in 20.9% (9/43) of UWS patients,

who also had a higher chance of recovery at 6 months [17]. Here, we evaluated whether these patients could also be identified by PCI^{ST}. The new index calculated on both high-density and standard 10–20 EEG setups detected all (n = 9) the patients with high PCI^{LZ}, whereas more than 82% of patients classified as low-complexity by PCI^{LZ} were also below threshold for PCI^{ST} (hd-EEG: 88.2%, 10–20 setup: 82.3%,
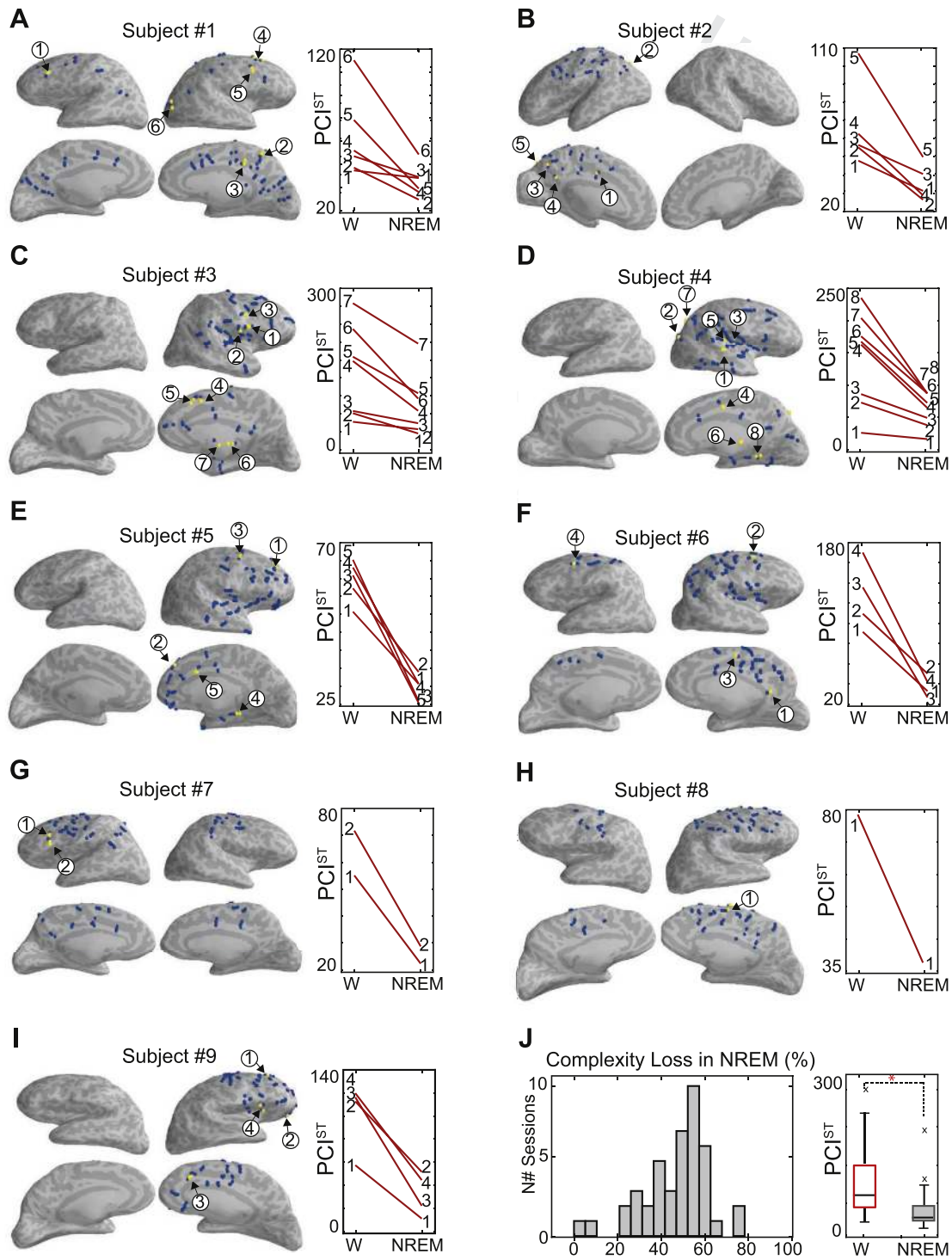
Fig. 5. PCI^{ST} values in SPES-evoked potentials are invariably lower during NREM sleep as compared to wakefulness. Panels A–I: PCI^{ST} calculated in nine subjects during wakefulness (W) and NREM sleep are shown separately for each individual subject. SEEG (blue) and SPES contacts (yellow) are depicted over brain surfaces reconstructed from the individual's brain (left). Numbers and arrows indicate the stimulation sites and the correspondent PCI^{ST} values (red traces, right). Panel J: shown are the percentage losses of complexity across all subjects and stimulation sites (left) and boxplots of PCI^{ST} values (right) at the group level for wakefulness (red box) and NREM sleep (grey box). Red asterisks indicate significant comparison ($p = 1.4 \times 10^{-7}$). (For interpretation of the references to colour in this figure legend, the reader is referred to the Web version of this article.)

Fig. 3B-top and middle). The simpler 8-channels setup detected 8 out of 9 (88.9%) high-complexity patients and 29 out of 34 (85.3%) low-complexity patients (Fig. 3B, bottom).

Taken together, these results show that PCIST calculation can afford an accurate, reliable and fast estimation of perturbational complexity at the sensor level even on reduced EEG set-ups. Combined with future optimizations of TMS-EEG hardware, this may allow the implementation of a practical method to be applied in real-time in the context of routine clinical setting.

PCIST reveals consistent changes of spatiotemporal complexity in intracranial recordings

Beside its practical applications, the estimation of perturbational complexity using different recording and stimulation protocols may allow for the exploration of the brain's causal structure across different scales, thus validating and extending the results of macroscopic TMS/EEG measurements, towards mesoscopic LFP and, in principle, microscopic multisite electrophysiological/optical responses. The development of PCIST allowed a first exploration of this possibility by estimating perturbational complexity on sparse intracranial SPES-evoked potentials. Specifically, we tested whether the state-dependent changes in complexity revealed at the macroscale by TMS/EEG could be reproduced at the mesoscale by intracranial electrical stimulation combined with SEEG recordings collected during wakefulness and sleep.

During wakefulness, the composite set of waves elicited by SPES resulted in a large number of components characterized by recurrent waves of activity lasting up to 600 ms in the principal components space, yielding high PCIST values (Fig. 4A–C). On the other hand, during NREM sleep, when SPES evoked a stereotypical wave, a small number of components were enough to span most of the response (Fig. 4D–F). In addition, the few components that survived dimensionality reduction in NREM sleep showed fewer state transitions than the ones in wakefulness and accounted for a reduced PCIST value. These findings were reproducible across stimulation sites and consistent at the population level (Fig. 5). PCIST during NREM sleep was lower than in wakefulness for each one of the 42 different stimulation sites (Fig. 5A–I). Overall, compared to wakefulness, PCIST was reduced during NREM sleep on average by 47.2% (Fig. 5J) and significant at the group level (p = 1.4×10^{-7}).

A key advantage of SPES over TMS is that the former is not associated with concurrent auditory and/or somatosensory stimulation [50]. The extent of the actual contribution of sensory co-stimulation to TEPs can be effectively minimized [51] but depends on many factors, such as coil type and effectiveness of noise masking, and is currently a matter of debate [51–54]. Hence, replicating fundamental TMS-EEG results using SPES-sEEG represents an important methodological step. Similarly to TMS, SPES elicited complex responses characterized by recurrent waves of activity both at short and long latencies in wakefulness and a stereotypical large-amplitude slow wave during NREM sleep (Figs. 4 and 5). In this respect, the present intracranial results provide a definite confirmation of the fundamental interpretation of perturbational complexity originally derived through TEPs, as a genuine index of state-dependent changes in intracortical interactions [55].

Furthermore, since with SPES/SEEG one can activate and record from smaller populations of neurons throughout the brain, which are not otherwise accessible to TMS/EEG, it would be important to explore regional differences in brain complexity. In this regard, the observed within-subject differences in the absolute values of PCIST in the SPES/SEEG recordings (Fig. 5) may reflect the presence of local anatomo-functional differences in the specific network engaged by the stimulation. Future analysis on larger datasets [56] as well as measurements in which SPES/SEEG is combined with whole brain macroscale recordings [57,58] may refine our understanding of the role of local nodes and circuits in the in the emergence of complex cortico-cortical interactions.

Most important, the application of PCIST across different brain scales may allow for the exploration of the neuronal mechanisms of global brain state changes. Indeed, the mesoscale assessment of perturbational complexity is in an ideal position to link microscale explorations at the bench to the macroscale measurements performed at the bedside of brain-injured patients. Connecting these levels is important as experiments in cortical slices [27], sleeping subjects and brain-injured patients [31] suggest that loss of brain complexity is linked to the tendency of neurons to enter a silent period upon an initial activation (OFF-period).

In the future, PCIST measurements applied to multiscale data including neuronal recordings could be used to inform experimental and computational models [59] aimed at devising novel interventions to restore complexity and thus consciousness following brain injury.

Conclusion

In this paper we have introduced, validated and tested PCIST, a method of estimating perturbational complexity based on dimensionality reduction and state-transitions quantification. The novel index may provide a reliable, fast and potentially online option for the assessment of consciousness in the clinical setting, achievable even with standard EEG systems. Furthermore, PCIST could also serve as a general translational tool for exploring the mechanisms of loss and recovery of brain complexity across species, scales, and models.

Funding

Conflicts of interest

None.

Acknowledgments

Appendix A. Supplementary data

Supplementary data to this article can be found online at https://doi.org/10.1016/j.brs.2019.05.013.

References

[1] Bassett DS, Bullmore ET. Human brain networks in health and disease. Curr Opin Neurol 2009;22(4):340–7.

[2] Deco G, Tononi G, Boly M, Kringelbach ML. Rethinking segregation and integration: contributions of whole-brain modelling. Nat Rev Neurosci 2015;16(7):430–9.

[3] Seth AK, Barrett AB, Barnett L. Causal density and integrated information as measures of conscious level. Philos Trans A Math Phys Eng Sci 2011;369(1952):3748–67.

[4] Sporns O, Tononi G, Edelman GM. Connectivity and complexity: the relationship between neuroanatomy and brain dynamics. Neural Network 2000;13(8–9):909–22.

[5] Tononi G, Boly M, Massimini M, Koch C. Integrated information theory: from consciousness to its physical substrate. Nat Rev Neurosci 2016;17(7):450–61.

[6] Tononi G, Edelman GM. Consciousness and complexity. Science 1998;282(5395):1846–51.

[7] Barrett AB, Murphy M, Bruno MA, Noirhomme Q, Boly M, Laureys S, et al. Granger causality analysis of steady-state electroencephalographic signals during propofol-induced anaesthesia. PLoS One 2012;7(1):e29072.

[8] Jobst BM, Hindriks R, Laufs H, Tagliazucchi E, Hahn G, Ponce-Alvarez A, et al. Increased stability and breakdown of brain effective connectivity during slow-wave sleep: mechanistic insights from whole-brain computational modelling. Sci Rep 2017;7(1):4634.

[9] Schartner M, Seth A, Noirhomme Q, Boly M, Bruno MA, Laureys S, et al. Complexity of multi-dimensional spontaneous EEG decreases during propofol induced general anaesthesia. PLoS One 2015;10(8):e0133532.

[10] Solovey G, Alonso LM, Yanagawa T, Fujii N, Magnasco MO, Cecchi GA, et al. Loss of consciousness is associated with stabilization of cortical activity. J Neurosci 2015;35(30):10866–77.

[11] Chennu S, Annen J, Wannez S, Thibaut A, Chatelle C, Cassol H, et al. Brain networks predict metabolism, diagnosis and prognosis at the bedside in disorders of consciousness. Brain 2017;140(8):2120–32.

[12] Gosseries O, Schnakers C, Ledoux D, Vanhaudenhuyse A, Bruno MA, Demertzi A, et al. Automated EEG entropy measurements in coma, vegetative state/unresponsive wakefulness syndrome and minimally conscious state. Funct Neurol 2011;26(1):25–30.

[13] Rosanova M, Gosseries O, Casarotto S, Boly M, Casali AG, Bruno MA, et al. Recovery of cortical effective connectivity and recovery of consciousness in vegetative patients. Brain 2012;135(Pt 4):1308–20.

[14] Sitt JD, King JR, El Karoui I, Rohaut B, Faugeras F, Gramfort A, et al. Large scale screening of neural signatures of consciousness in patients in a vegetative or minimally conscious state. Brain 2014;137(Pt 8):2258–70.

[15] Thul A, Lechinger J, Donis J, Michitsch G, Pichler G, Kochs EF, et al. EEG entropy measures indicate decrease of cortical information processing in disorders of consciousness. Clin Neurophysiol 2016;127(2):1419–27.

[16] Casali AG, Gosseries O, Rosanova M, Boly M, Sarasso S, Casali KR, et al. A theoretically based index of consciousness independent of sensory processing and behavior. Sci Transl Med 2013;5(198):198ra05.

[17] Casarotto S, Comanducci A, Rosanova M, Sarasso S, Fecchio M, Napolitani M, et al. Stratification of unresponsive patients by an independently validated index of brain complexity. Ann Neurol 2016;80(5):718–29.

[18] Sarasso S, Boly M, Napolitani M, Gosseries O, Charland-Verville V, Casarotto S, et al. Consciousness and complexity during unresponsiveness induced by propofol, xenon, and ketamine. Curr Biol 2015;25(23):3099–105.

[19] Hallez H, Vanrumste B, Grech R, Muscat J, De Clercq W, Vergult A, et al. Review on solving the forward problem in EEG source analysis. J NeuroEng Rehabil 2007;4:46.

[20] Baillet SMJC, Leahy RM. Electromagnetic brain mapping. IEEE Signal Process Mag 2001:14–30. November.

[21] Lewis LD, Weiner VS, Mukamel EA, Donoghue JA, Eskandar EN, Madsen JR, et al. Rapid fragmentation of neuronal networks at the onset of propofol-induced unconsciousness. Proc Natl Acad Sci U S A 2012;109(49):E3377–86.

[22] Pigorini A, Sarasso S, Proserpio P, Szymanski C, Arnulfo G, Casarotto S, et al. Bistability breaks-off deterministic responses to intracortical stimulation during non-REM sleep. Neuroimage 2015;112:105–13.

[23] Bettinardi RG, Tort-Colet N, Ruiz-Mejias M, Sanchez-Vives MV, Deco G. Gradual emergence of spontaneous correlated brain activity during fading of general anesthesia in rats: evidences from fMRI and local field potentials. Neuroimage 2015;114:185–98.

[24] Olcese U, Bos JJ, Vinck M, Lankelma JV, van Mourik-Donga LB, Schlumm F, et al. Spike-based functional connectivity in cerebral cortex and Hippocampus: loss of global connectivity is coupled to preservation of local connectivity during non-REM sleep. J Neurosci 2016;36(29):7676–92.

[25] Vyazovskiy VV, Faraguna U, Cirelli C, Tononi G. Triggering slow waves during NREM sleep in the rat by intracortical electrical stimulation: effects of sleep/wake history and background activity. J Neurophysiol 2009;101(4):1921–31.

[26] Vyazovskiy VV, Olcese U, Cirelli C, Tononi G. Prolonged wakefulness alters neuronal responsiveness to local electrical stimulation of the neocortex in awake rats. J Sleep Res 2013;22(3):239–50.

[27] D'Andola M, Rebollo B, Casali AG, Weinert JF, Pigorini A, Villa R, et al. Bistability, causality, and complexity in cortical networks: an in vitro perturbational study. Cerebr Cortex 2017:1–10.

[28] Sanchez-Vives MV, Massimini M, Mattia M. Shaping the default activity pattern of the cortical network. Neuron 2017;94(5):993–1001.

[29] Storm JF, Boly M, Casali AG, Massimini M, Olcese U, Pennartz CMA, et al. Consciousness regained: disentangling mechanisms, brain systems, and behavioral responses. J Neurosci 2017;37(45):10882–93.

[30] Mutanen T, Nieminen JO, Ilmoniemi RJ. TMS-evoked changes in brain-state dynamics quantified by using EEG data. Front Hum Neurosci 2013;7:155.

[31] Rosanova M, Fecchio M, Casarotto S, Sarasso S, Casali AG, Pigorini A, et al. Sleep-like cortical OFF-periods disrupt causality and complexity in the brain of unresponsive wakefulness syndrome patients. Nat Commun 2018;9(1):4427.

[32] Chassoux F, Navarro V, Catenoix H, Valton L, Vignal JP. Planning and management of SEEG. Neurophysiol Clin 2018;48(1):25–37.

[33] Cossu M, Cardinale F, Castana L, Citterio A, Francione S, Tassi L, et al. Stereo-electroencephalography in the presurgical evaluation of focal epilepsy: a retrospective analysis of 215 procedures. Neurosurgery 2005;57(4):706–18. discussion -18.

[34] Isnard J, Taussig D, Bartolomei F, Bourdillon P, Catenoix H, Chassoux F, et al. French guidelines on stereoelectroencephalography (SEEG). Neurophysiol Clin 2018;48(1):5–13.

[35] Prime D, Rowlands D, O'Keefe S, Dionisio S. Considerations in performing and analyzing the responses of cortico-cortical evoked potentials in stereo-EEG. Epilepsia 2018;59(1):16–26.

[36] Fischl B. FreeSurfer. Neuroimage 2012;62(2):774–81.

[37] Arnulfo G, Narizzano M, Cardinale F, Fato MM, Palva JM. Automatic segmentation of deep intracerebral electrodes in computed tomography scans. BMC Bioinf 2015;16:99.

[38] Valentin A, Anderson M, Alarcon G, Seoane JJ, Selway R, Binnie CD, et al. Responses to single pulse electrical stimulation identify epileptogenesis in the human brain in vivo. Brain 2002;125(Pt 8):1709–18.

[39] Cash SS, Halgren E, Dehghani N, Rossetti AO, Thesen T, Wang C, et al. The human K-complex represents an isolated cortical down-state. Science 2009;324(5930):1084–7.

[40] Li G, Jiang S, Paraskevopoulou SE, Wang M, Xu Y, Wu Z, et al. Optimal referencing for stereo-electroencephalographic (SEEG) recordings. Neuroimage 2018;183:327–35.

[41] Chang JY, Pigorini A, Massimini M, Tononi G, Nobili L, Van Veen BD. Multivariate autoregressive models with exogenous inputs for intracerebral responses to direct electrical stimulation of the human brain. Front Hum Neurosci 2012;6:317.

[42] Axmacher N, Henseler MM, Jensen O, Weinreich I, Elger CE, Fell J. Cross-frequency coupling supports multi-item working memory in the human hippocampus. Proc Natl Acad Sci U S A 2010;107(7):3228–33.

[43] Bragin A, Jando G, Nadasdy Z, Hetke J, Wise K, Buzsaki G. Gamma (40-100 Hz) oscillation in the hippocampus of the behaving rat. J Neurosci 1995;15(1 Pt 1):47–60.

[44] Canolty RT, Edwards E, Dalal SS, Soltani M, Nagarajan SS, Kirsch HE, et al. High gamma power is phase-locked to theta oscillations in human neocortex. Science 2006;313(5793):1626–8.

[45] Lisman JE, Jensen O. The theta-gamma neural code. Neuron 2013;77(6):1002–16.

[46] Young CK, Eggermont JJ. Coupling of mesoscopic brain oscillations: recent advances in analytical and theoretical perspectives. Prog Neurobiol 2009;89(1):61–78.

[47] Marwan N, Carmen Romano M, Thiel M, Kurths J. Recurrence plots for the analysis of complex systems. Phys Rep 2007;438:237–329.

[48] Webber Jr CL, Zbilut JP. Dynamical assessment of physiological systems and states using recurrence plot strategies. J Appl Physiol 1985;76(2):965–73. 1994.

[49] Pedregosa F, Varoquaux G, Gramfort A, Michel V, Thirion B, Grisel O. Scikit-learn: machine learning in python. J Mach Learn Res 2011;12:2825–30.

[50] Nikouline V, Ruohonen J, Ilmoniemi RJ. The role of the coil click in TMS assessed with simultaneous EEG. Clin Neurophysiol 1999;110(8):1325–8.

[51] Gosseries O, Sarasso S, Casarotto S, Boly M, Schnakers C, Napolitani M, et al. On the cerebral origin of EEG responses to TMS: insights from severe cortical lesions. Brain Stimul 2015;8(1):142–9.

[52] Biabani M, Fornito A, Mutanen TP, Morrow J, Rogasch NC. Characterizing and minimizing the contribution of sensory inputs to TMS-evoked potentials. BioRxiv (preprint) https://doi.org/10.1101/489864_2018.

[53] Conde V, Tomasevic L, Akopian I, Stanek K, Saturnino GB, Thielscher A, et al. The non-transcranial TMS-evoked potential is an inherent source of ambiguity in TMS-EEG studies. Neuroimage 2018;185:300–12.

[54] Gordon PC, Desideri D, Belardinelli P, Zrenner C, Ziemann U. Comparison of cortical EEG responses to realistic sham versus real TMS of human motor cortex. Brain Stimul 2018;11(6):1322–30.

[55] Chang JY, Fecchio M, Pigorini A, Massimini M, Tononi G, Van Veen BD. Assessing recurrent interactions in cortical networks: modeling EEG response to transcranial magnetic stimulation. J Neurosci Methods 2019;312:93–104.

[56] David O, Job AS, De Palma L, Hoffmann D, Minotti L, Kahane P. Probabilistic functional tractography of the human cortex. Neuroimage 2013;80:307–17.

[57] Dubarry AS, Badier JM, Trebuchon-Da Fonseca A, Gavaret M, Carron R, Bartolomei F, et al. Simultaneous recording of MEG, EEG and intracerebral EEG during visual stimulation: from feasibility to single-trial analysis. Neuroimage 2014;99:548–58.

[58] Pizzo F, Roehri N, Medina Villalon S, Trebuchon A, Chen S, Lagarde S, et al. Deep brain activities can be detected with magnetoencephalography. Nat Commun 2019;10(1):971.

[59] Deco G, Cabral J, Saenger VM, Boly M, Tagliazucchi E, Laufs H, et al. Perturbation of whole-brain dynamics in silico reveals mechanistic differences between brain states. Neuroimage 2018;169:46–56.